Available online at www.sciencedirect.com
ScienceDirect
Journal of the European Ceramic Society 31 (2011) 2393–2400
www.elsevier.com/locate/jeurceramsoc

Anomalous oxidation behaviour of pressureless liquid-phase-sintered SiC

F. Rodríguez-Rojas [a], A.L. Ortiz [a,*], F. Guiberteau [a], M. Nygren [b]

[a] *Departamento de Ingeniería Mecánica, Energética y de los Materiales, Universidad de Extremadura, 06071 Badajoz, Spain*
[b] *Department of Materials and Environmental Chemistry, University of Stockholm, 10691 Stockholm, Sweden*

Received 31 January 2011; received in revised form 29 April 2011; accepted 13 May 2011
Available online 14 June 2011

Abstract

The oxidation behaviour of pressureless liquid-phase-sintered (PLPS) SiC, an important non-oxide engineering ceramic, was investigated, and was found to be universally anomalous. Thermogravimetry oxidation tests performed in oxygen in the temperature range 1000–1225 °C on three PLPS SiC ceramics fabricated with different combinations of Al_2O_3–RE_2O_3 (RE = Gd, Sc, or Sm) as sintering aids indicated that the oxidation is in all cases passive and protective, but unexpectedly anomalous in the sense that the oxidation resistance does not scale inversely with temperature. In particular, in all cases it was observed that there is less oxidation above 1100 °C than below, in clear contradiction to the expectation for a diffusional process. Exhaustive characterization of the oxide scales by scanning electron microscopy, X-ray energy dispersive spectrometry, and X-ray diffractometry, together with detailed modeling of the oxidation curves, showed that the origin of this universal anomalous oxidation behaviour lies in the marked crystallization within the oxide scale of rare-earth silicates that act as effective barriers against the inward diffusion of oxygen thus improving notably the oxidation resistance. A strategy is proposed to provide PLPS SiC, and probably other SiO_2-scale-forming ceramics that are sintered using rare-earth oxides, with the superior oxidation resistance at moderate temperatures (i.e., <1100 °C) that they do not currently have.

Keywords: D. SiC; Liquid-phase sintering; Oxidation

1. Introduction

Non-oxide advanced ceramics are increasingly being used in engineering applications at high temperature in air or other oxidizing atmospheres.[1] Oxidation is thus a major cause of their degradation in service,[2,3] and the oxidation behaviour of non-oxide engineering ceramics is currently a topic of intensive research and a critical aspect of design. Pressureless liquid-phase-sintered (PLPS) SiC is one of these non-oxide engineering ceramics with great potential for high-temperature structural and functional applications because it combines a very attractive set of physicochemical properties with the economy and ease of the pressureless processing for the fabrication of large components with complex geometries. Current opinion is that PLPS SiC can operate safely in oxidizing environments below ~1300 °C because up to that temperature the oxide scales that form are protective, and the oxidation is passive and is controlled by diffusion.[4] In addition, because the diffusion coefficients obey an Arrhenius-type law, the conventional wisdom within the ceramic community and among design engineers is that the oxidation resistance of PLPS SiC decreases with increasing temperature in the temperature range 25–1300 °C. Indeed, the history of literature on the oxidation of LPS SiC ceramics, pressureless processed or not, long presented no evidence against this wisdom,[4–17 *and references therein*]. However, an oxidation study by Jensen et al.[18] on a PLPS SiC fabricated with 20 vol% Y_2O_3–Al_2O_3 (henceforth, PLPS SiC–Y) showed clear evidence, although the only case published so far, contradicting the common belief that the oxidation resistance scales inversely with temperature. In particular, they oxidized their PLPS SiC–Y ceramic in ambient air between 1000 and 1350 °C, observing surprisingly greater oxidation at 1000 °C than at 1100, 1150, 1200, and 1250 °C, an unexpected phenomenon that they confirmed by repeated oxidation tests. This oxidation behaviour is highly anomalous not only because the oxygen diffusivity

* Corresponding author. Tel.: +34 924289600×86726; fax: +34 924289601.
E-mail addresses: alortiz@materiales.unex.es, alortiz@unex.es (A.L. Ortiz).

0955-2219/$ – see front matter © 2011 Elsevier Ltd. All rights reserved.
doi:10.1016/j.jeurceramsoc.2011.05.015

increases by two or more orders of magnitude in 250 °C, but also because they found no signs of formation of non-protective oxide scales. Indeed, the origin of such anomalous oxidation behaviour has yet to be elucidated. Furthermore, while the study of Jensen et al. does not necessarily imply universality, the fact that the microstructural ingredients are essentially the same in all PLPS SiC ceramics[4] suggests that the anomalous oxidation behaviour observed in the PLPS SiC–Y ceramic might not be exclusive to that type but may also occur in all other PLPS SiC ceramics fabricated with other rare-earth oxides. Whether or not this anomalous oxidation is universal in PLPS SiC's is a fundamental question requiring an answer, as it may have important consequences for the use of these ceramics in high-temperature applications in oxidizing atmospheres. If the phenomenon indeed turned out to be universal, then there arise two fundamental questions: What is its origin, and how can it be prevented?

The present study seeks to address these issues. To this end, we fabricated three PLPS SiC ceramics with Al_2O_3–RE_2O_3 (RE = Gd, Sc, or Sm; henceforth, PLPS SiC–RE) as sintering additives, and oxidized them at different temperatures. We also observed in these three PLPS SiC ceramics the anomalous oxidation of the PLPS SiC–Y ceramic. We next went a step further and identified in the PLPS SiC–Gd ceramic the origin of the anomalous oxidation by an exhaustive characterization of the oxide scales through scanning electron microscopy (SEM), X-ray energy dispersive spectrometry (XEDS), and X-ray diffractometry (XRD), together with a detailed analytical modeling of the oxidation curves, and then validated the findings in the PLPS SiC–Sc and –Sm ceramics. Based on the experimental results and analyses, we propose a strategy to provide PLPS SiC with superior oxidation resistance at moderate temperatures (i.e., <1100 °C), which can have important implications for its use in applications requiring oxidation-resistance.

2. Experimental procedure

The processing procedure used is that employed conventionally to fabricate PLPS SiC ceramics. Commercially available α-SiC (UF-15, H.C. Starck, Goslar, Germany), Al_2O_3 (AKP-30, Sumitomo Chemical Company, Japan), and RE_2O_3 (Gd_2O_3, Sc_2O_3, and Sm_2O_3; Strem Chemicals, France) powders were used as starting materials. The choice of these rare-earth oxides is because they allow one to investigate the fundamental questions of the universality of the anomalous oxidation observed in the PLPS SiC–Y ceramic and its origin if such universality is indeed the case, while contributing new data to the PLPS SiC oxidation literature. Three powder batches were individually prepared by combining the SiC, Al_2O_3, and RE_2O_3 (RE = Gd, Sc, or Sm) powders in appropriate amounts to result in PLPS SiC ceramics with 90 vol.% SiC and 10 vol.% $RE_3Al_5O_{12}$ after sintering (henceforth abbreviated as PLPS SiC–RE). The powder mixtures were then blended intimately by wet ball milling in ethanol for 24 h in polyethylene bottles using Si_3N_4 balls as milling media. The resulting slurries were dried carefully in Teflon beakers on hot-plates while being continuously stirred, and subsequently in an oven at 100 °C for 24 h. The dried powders were next crushed and sieved to remove the hard agglomerates. Compacts were then made from each of the powder batches by uniaxial pressing (C, Carver Inc., Wabash, IN, USA) at 50 MPa, followed by cold-isostatic pressing (CP360, AIP, Columbus, OH, USA) at 350 MPa. Finally, the individual pellets were embedded in powder beds inside graphite crucibles and were pressureless sintered in a graphite furnace (1000-3560-FP20, Thermal Technology Inc., Santa Rosa, CA, USA) at 1950 °C for 1 h in a flowing Ar-gas atmosphere of 99.999% purity. The sintered materials were ground down 1 mm and polished to a 1-μm finish, and their microstructure was examined by SEM (S-3600N, Hitachi, Japan) after plasma etching with $CF_4 + 4\%O_2$ gas for 2 h.

Parallelepiped specimens of size 8 mm × 5 mm × 2 mm were machined out of the sintered discs and all their faces were diamond-polished to a 1-μm finish. The oxidation tests were carried out with a thermobalance (TAG 24, Setaram, France) whose resolution is better than 2 μg and whose baseline drift is lower than 5 μg per 24 h. The oxidation tests were performed at different temperatures (1000, 1150 and 1225 °C for PLPS SiC–Gd, 1075 and 1225 °C for PLPS SiC–Sc, and 1075 and 1150 °C for PLPS SiC–Sm), in an atmosphere of flowing (50 mL/min) dry oxygen of 99.999% purity, for times in the range 0–22 h, and with the specimens suspended on the thermobalance by Pt wires. The oxidized samples were characterized as extracted from the thermobalance by SEM, XEDS (XFLASH Detector 3001, Röntec GmbH, Germany), and XRD (X'pert PRO MPD, PANalytical, The Netherlands) to determine the microstructure and chemical composition (elemental and crystalline phases) of the oxide scales. The surface coverage of the oxide scales by crystals was also measured, by image analysis of the SEM micrographs.

3. Results and discussion

Fig. 1 shows representative SEM micrographs of the three PLPS SiC–RE ceramics in the as-processed condition. As can be seen, they all have the microstructure typical of PLPS SiC ceramics, with submicrometre SiC grains (∼0.8 μm) embedded in a continuous oxide matrix. The aspect ratio of the SiC grains is 1.4, which is the equilibrium morphology of α-SiC.[19] It can also be seen that the three ceramics are fully dense because there is no evidence of residual porosity in the SEM images.

Fig. 2 shows the specific mass-change curves measured experimentally for the three PLPS SiC–RE ceramics oxidized at different temperatures. As can be observed, in the three cases there is always mass gain throughout the oxidation period, which indicates that the oxidation is passive due to the formation of oxide scales. This is consistent with the fact that the active oxidation of PLPS SiC occurs at lower oxygen partial pressure and higher temperatures than used in the present study[2]. A detailed inspection of the oxidation curves in Fig. 2 reveals nevertheless that the oxidation behaviour of the three PLPS SiC–RE ceramics is highly anomalous, as will be described in the following. As can be seen in Fig. 2A for the PLPS SiC–Gd ceramic, initially both the rate of specific mass gain and the total specific mass gain at 1000 °C are lower than at 1150 and 1225 °C. After ∼0.5 h of oxidation this scenario changes partly, so that the rate of spe-

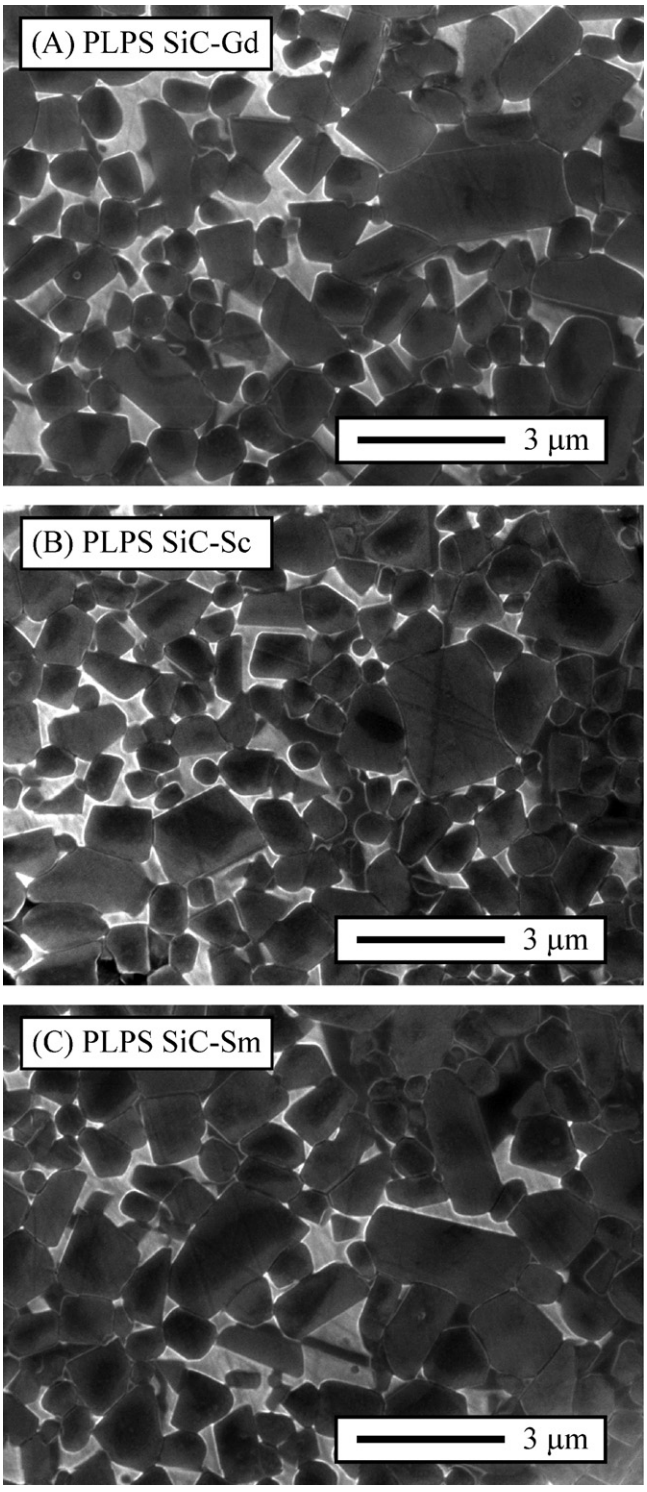

Fig. 1. SEM images (taken with secondary electrons) of the polished and plasma-etched microstructures of the PLPS SiC ceramics fabricated with sintering aids (10 vol.%) of: (A) Al_2O_3–Gd_2O_3, (B) Al_2O_3–Sc_2O_3, and (C) Al_2O_3–Sm_2O_3.

cific mass gain now becomes lower at 1150 and 1225 °C than at 1000 °C, although the total specific mass gain at 1000 °C is still lower. After ~2 h of oxidation there is already less total specific mass gain at 1150 °C than at 1000 °C, a fact that also occurs after ~3.5 h of oxidation for 1225 °C. However, the rate of specific mass gain at 1150 °C is always lower than at 1225 °C. Following Jensen et al.,[18] we also repeated the oxidation test at 1000 °C and observed no differences between the two tests. It can also be seen in Fig. 2B that the PLPS SiC–Sc ceramic exhibits the same oxidation behaviour as the PLPS SiC–Gd ceramic, with the inversion in the rate of specific mass gain and in the total specific mass gain between 1075 and 1225 °C occurring after ~1 and 3 h of oxidation, respectively. Finally, one observes in Fig. 2C that the PLPS SiC–Sm ceramic exhibits an oxidation behaviour analogous to that of the PLPS SiC–Gd and –Sc ceramics, with the exception that the rate of specific mass gain and the total specific mass gain are both greater at 1075 °C than at 1150 °C from the beginning of the oxidation. Clearly, all these trends and that observed before by Jensen et al.[18] are not what is expected, and highlight that the oxidation behaviour of the PLPS SiC ceramics is both quite complicated and unusual, and certainly universal. In what follows we shall first explore the origin of this anomalous oxidation behaviour in the PLPS SiC–Gd ceramic, and then check for confirmation that the conclusions drawn are also valid for the PLPS SiC–Sc and –Sm ceramics.

Consider again the oxidation curves of the PLPS SiC–Gd ceramic in Fig. 2A. Two possible explanations immediately suggest themselves for the anomalous oxidation behaviour observed. The first is that the oxide scale could be protective at 1150 and 1225 °C but not at 1000 °C due to the presence of cracks, which would explain the poorer oxidation resistance at 1000 °C. And the second is that the oxide scale could be protective at 1000 °C but only semi-protective at 1150 and 1225 °C, so that the PLPS SiC–Gd ceramic is indeed less resistant to the oxidation at these two temperatures, while the corresponding oxidation curves are substantially below that at 1000 °C due to the concurrence of processes of gain and loss of specific mass. However, the analysis of the oxidation curves and the SEM observations of the oxide scales indicate that neither of these potential explanations can be correct. Firstly, if the oxide scale that forms at 1000 °C were non-protective due to the presence of cracks, the oxidation kinetics would not be curved as observed experimentally but linear because the oxidation rate would be dictated by the speed of the interfacial reaction $2SiC(s) + 3O_2(g) \rightarrow 2SiO_2(s) + 2CO(g)$ since the SiC grains underneath the oxide scale would be in permanent direct contact with the oxidizing atmosphere.[16] In addition, cracks were never observed during the SEM examination of the oxide scale developed at 1000 °C. Therefore, the oxidation behaviour at 1000 °C cannot be catalogued as non-protective passive. And secondly, if the oxide scales that form at 1150 and 1225 °C were only semi-protective the corresponding oxidation kinetics would be paralinear, and the oxidation curves would bend significantly downward for the greater oxidation times when the recession term of the oxide scale $-k_l t$ dominates over the growth term $(k_p t)^{1/2}$.[16] However, no such concavity is observed in the $(\Delta m_s)^2 - t$ plots. Furthermore, the SEM observations of the oxide scale developed at 1150 and 1225 °C showed no signs of formation of liquid oxidation products that flow out of the sample. Formation of low-viscosity liquid phases has been observed before during the oxidation of PLPS SiC,[16,17,20] but not at oxidizing temperatures as low as 1150 °C because the eutectic

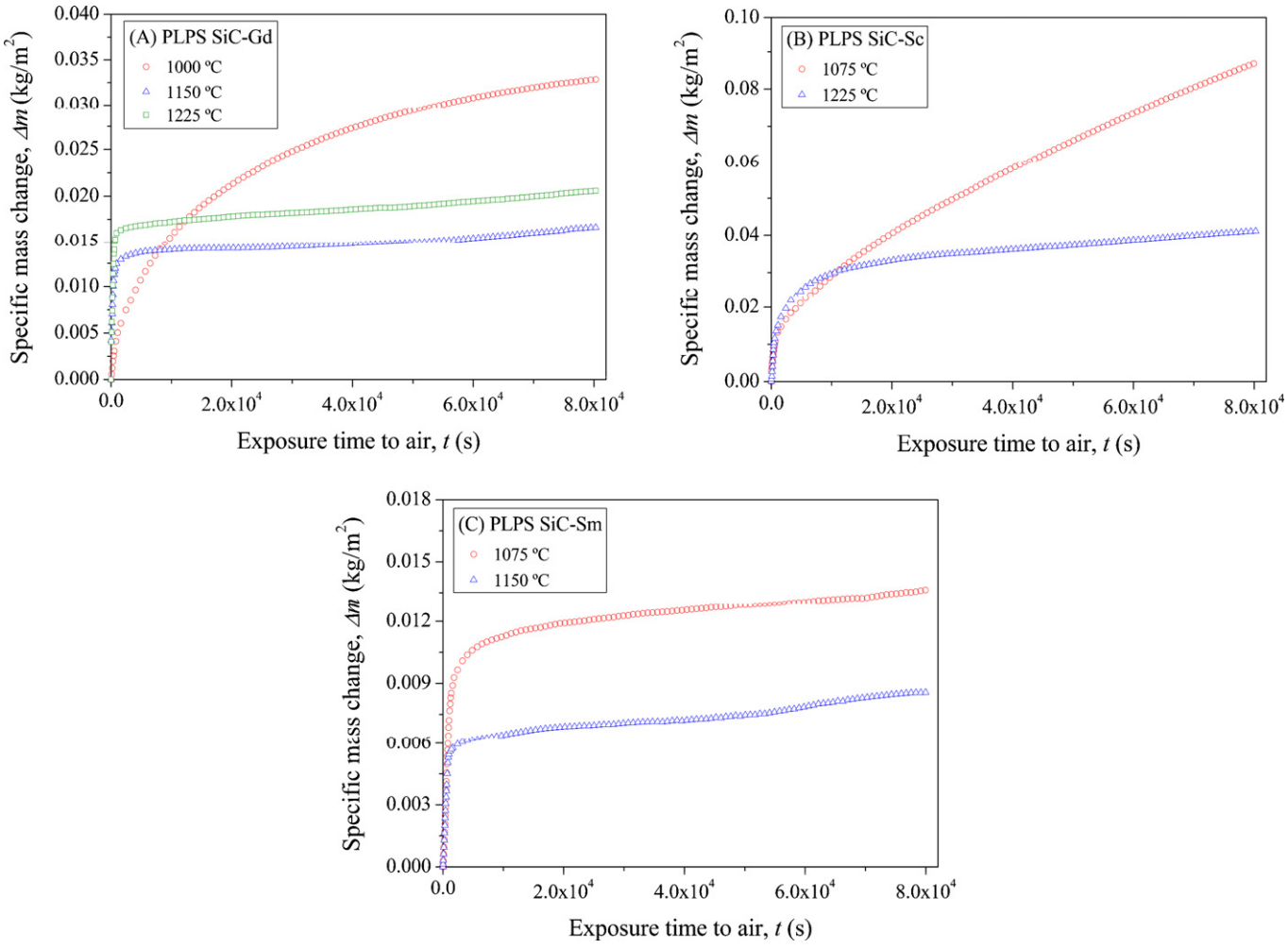

Fig. 2. Oxidation curves in oxygen of the three ceramics prepared in this study: (A) PLPS SiC–Gd, (B) PLPS SiC–Sc, and (C) PLPS SiC–Sm.

temperatures in the Al_2O_3–RE_2O_3 or SiO_2–RE_2O_3 binary systems and in the SiO_2–Al_2O_3–RE_2O_3 ternary systems are much higher. Therefore, the oxidation behaviour at 1150 and 1225 °C cannot be classified as semi-protective passive.

Given that the passive oxidation is protective at the three temperatures, it is therefore reasonable to think that the crystallization of the oxide scales may then well be the origin of the anomalous oxidation behaviour. Crystallization of rare-earth silicates during the oxidation of PLPS SiC is a well-known phenomenon,[4,7–17] and results in substantial improvements of their oxidation resistance (the greater the crystallization the greater the improvement) because the crystalline precipitates reduce the effective cross section available for inward diffusion of oxygen[2]. With this in mind, we propose that the greater oxidation resistance at 1150 and 1225 °C than at 1000 °C is due to the greater crystallization of the oxide scales predominating over the increase in the diffusion coefficient. This hypothesis was tested experimentally by characterizing the oxide scales by SEM, XEDS, and XRD. Shown in Fig. 3 are representative plane-view SEM micrographs of the PLPS SiC–Gd ceramic after oxidation at 1000, 1150, and 1225 °C for 22 h. As can be observed in Fig. 3A, the oxide scale at 1000 °C contains small crystals, but the surface coverage by these crystals is only ∼30%. In contrast, Fig. 3B shows that the oxide scale at 1150 °C is markedly covered by larger crystals, with an estimated surface coverage of ∼70%. Finally, it can be seen in Fig. 3C that the oxidation at 1225 °C results in even greater surface crystallinity of the oxide scale (∼80%), but not much greater than that at 1150 °C despite the crystals now clearly being larger. The XEDS analysis indicated that these crystals have $Gd_2Si_2O_7$ stoichiometry, and that the amorphous matrix between the crystals is rich in silica, with some dissolved Gd and Al. Fig. 4 shows XRD patterns confirming the presence of peaks from $Gd_2Si_2O_7$ after oxidation (see the peaks between 25 and 32° 2θ), whose intensity increases with increasing oxidizing temperature but not at the expense of the intensity of the SiC peaks (compare the peak at ∼35.6° 2θ). Thus, the SEM, XEDS, and XRD analyses prove that the anomalous oxidation behaviour of the PLPS SiC–Gd ceramic is due to the marked crystallization of its oxide scales at 1150 and 1225 °C relative to 1000 °C. This finding is fully consistent with an earlier study of crystallization of various $RE_2Si_2O_7$ disilicates from RE_2O_3:SiO_2 mixtures,[21] which showed that they start to crystallize between 950 and 1100 °C and that the exact onset of crystallization depends slightly on the RE^{3+} cation in the rare-earth oxide. Hence, the anomalous oxidation of PLPS SiC, while universal, had not been observed regularly before

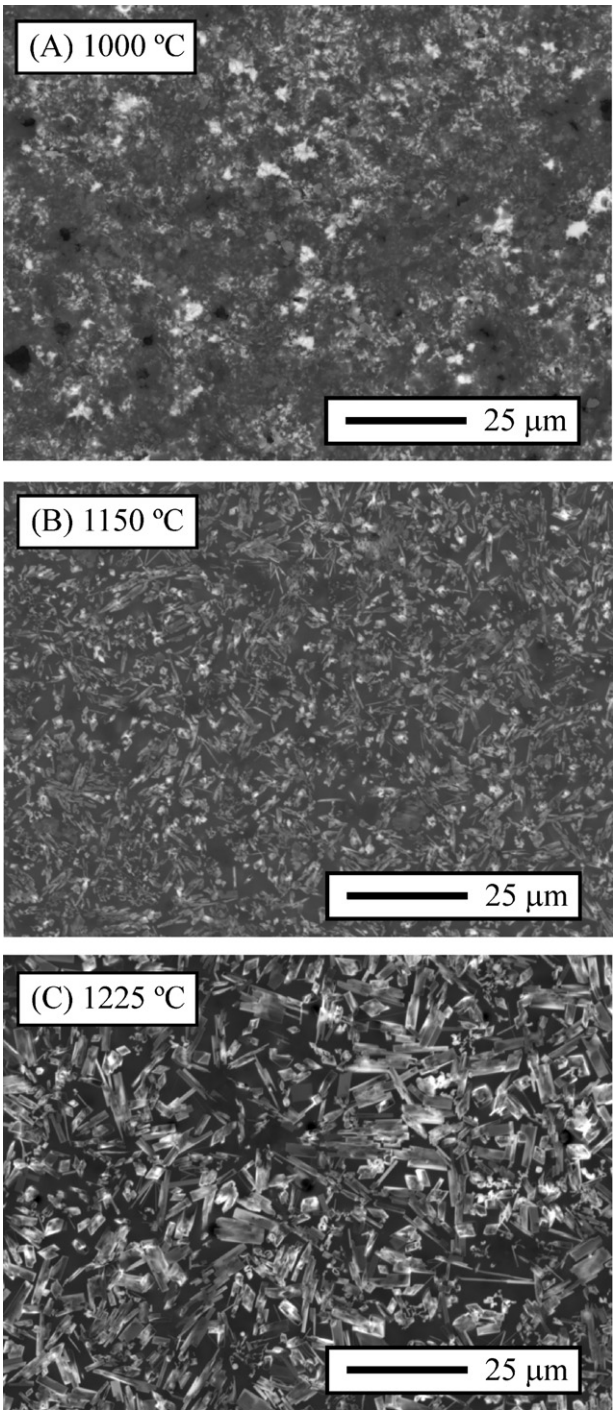

Fig. 3. Plane-view SEM micrographs (taken with backscattered electrons) of the PLPS SiC–Gd ceramic after oxidation in oxygen for 22 h at: (A) 1000 °C, (B) 1150 °C, and (C) 1225 °C.

simply because the oxidation studies on PLPS SiC use temperatures higher than ~950–1100 °C, below which there is little or no crystallization of $RE_2Si_2O_7$ disilicates. The lower oxidation resistance at 1225 °C than at 1150 °C is explained by considering that the slight increase in the surface coverage by crystals is insufficient to compensate for the increased diffusion coefficient.

To further support experimentally the conclusions drawn from the SEM, XEDS, and XRD analyses, the three oxidation curves were modeled by the typical parabolic-rate law $\Delta m_s=(k_p t)^{1/2}$, where Δm_s is the specific mass change, k_p the parabolic-rate constant, and t the oxidation time. This oxidation kinetics model is derived from Fick's first law, assuming that the cross section available for diffusion remains invariable throughout the oxidation period, and therefore is strictly applicable only when the oxide scale does not crystallize progressively during the exposure to the oxidizing atmosphere because the crystals act as an effective barrier against the inward diffusion of oxygen. In this scenario it is expected that: (i) the parabolic-rate law cannot satisfactorily capture any of the three oxidation curves because in the three cases there is crystallization of the oxide scale; and (ii) the fits are markedly poorer for the oxidation curves at 1150 and 1225 °C than at 1000 °C because in this last case the oxide scale is ~2.3–2.8 times less crystalline. This is exactly what is observed in Fig. 5, which shows the model curves determined by fitting the parabolic-rate law to the oxidation curves by the nonlinear least squares method. Thus, this analytical modeling

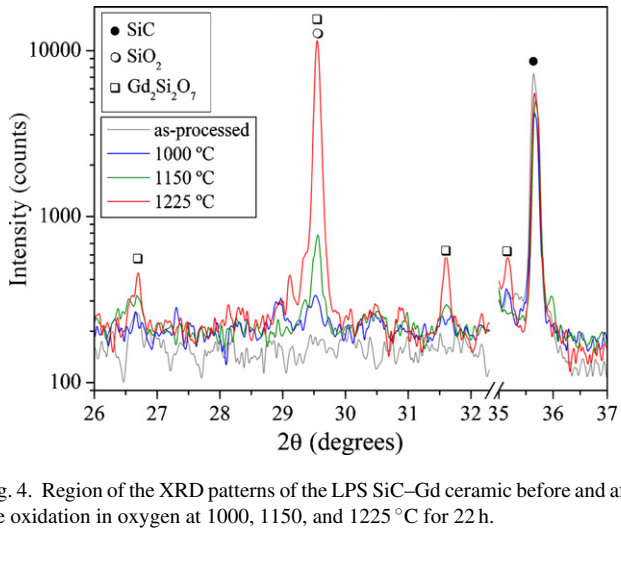

Fig. 4. Region of the XRD patterns of the LPS SiC–Gd ceramic before and after the oxidation in oxygen at 1000, 1150, and 1225 °C for 22 h.

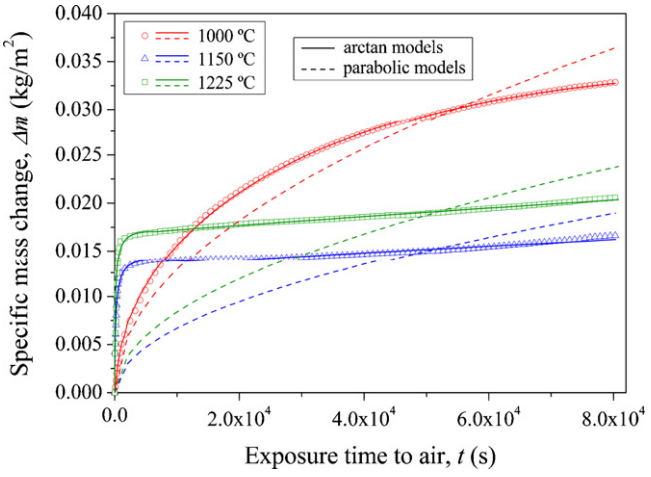

Fig. 5. Oxidation curves in oxygen of the PLPS SiC–Gd ceramic at 1000, 1150, and 1225 °C. The points are the experimental data, and the dashed and solid lines are the corresponding parabolic and arctan models of the oxidation kinetics (discussed in the text), respectively.

of the oxidation curves confirms that the origin of the anomalous oxidation lies in the crystallization of the oxide scales.

Another interesting aspect found during the modeling of the oxidation curves by the parabolic-rate law is that the resulting oxidation constants (1.6533×10^{-8}, 4.44845×10^{-9}, and $7.0337 \times 10^{-9}\,kg^2\,m^{-4}\,s^{-1}$ at 1000, 1150, and 1225 °C, respectively) not only are erroneous because the modeling of the oxidation kinetics is clearly unsatisfactory, but also violate the Arrhenius law that $Ln\,K_p$ should decrease linearly with increasing $1/T$, and therefore cannot even be used to roughly estimate the activation energy of the oxidation process. This fact was also observed in the oxidation study of the PLPS SiC-Y ceramic,[18] in which the strategy adopted to compute the activation energy of the oxidation was to exclude the parabolic-rate constant at 1000 °C from the calculations. This approach, however, does not eliminate the underlying problem of the poor modeling of the oxidation curves by the parabolic-rate law. The proper modeling of oxidation curves requires the adoption of a rate law that considers explicitly the crystallization of the oxide scales. The arctan-rate law is the modification of the parabolic-rate law for cases such as the present when the amorphous cross-section available for diffusion decreases progressively during oxidation.[2,4,16] It has the form:

$$\Delta m_s = \frac{\beta\sqrt{k_p}\,(1-f)}{\sqrt[3]{(\beta - 1/t_0)^2}} \arctan\sqrt{(\beta - 1/t_0)\,t} + \frac{\sqrt{k_p}\,(\beta f - 1/t_0)}{(\beta - 1/t_0)}\sqrt{t}$$

where Δm_s and k_p have the same meaning as before, and β is the rate constant for the decrease of the area, f the fraction of original area that still remains amorphous, and t_0 the time at which the crystallization process stops. Therefore, unlike the parabolic-rate law, the arctan-rate law should indeed capture the form of the three experimental oxidation curves well. As can be observed in Fig. 5, this is indeed the case (coefficients of determination of $R^2 = 0.999$, 0.988, and 0.984 for the oxidation curves of 1000, 1150 and 1225 °C). Details on the exact fitting protocol followed to model the oxidation curves by the arctan-rate law have been given elsewhere[4]. The fractions of the original area that still remain amorphous as calculated by the arctan-rate law for the oxidations at 1000, 1150, and 1225 °C are 69, 31, and 19%, respectively, which are in perfect agreement with the SEM observations. The rate constants for these oxidizing temperatures are 2.6×10^{-8}, 6.83×10^{-7}, and $1.473 \times 10^{-6}\,kg^2\,m^{-4}\,s^{-1}$, respectively. As expected for a diffusional process, these rate constants do increase with increasing oxidizing temperature, and also obey the Arrhenius law. Thus, they allow the measurement of the activation energy of the oxidation process, and the identification of its rate-limiting mechanism. The Arrhenius plot gave an activation energy of 292 ± 33 kJ/mol, a value that falls within the range of 250–600 kJ/mol associated with oxidation controlled by the outward diffusion of rare-earth cations (Gd^{3+} in the present case) from the secondary intergranular phase into the oxide scale.[4,6,12,14]

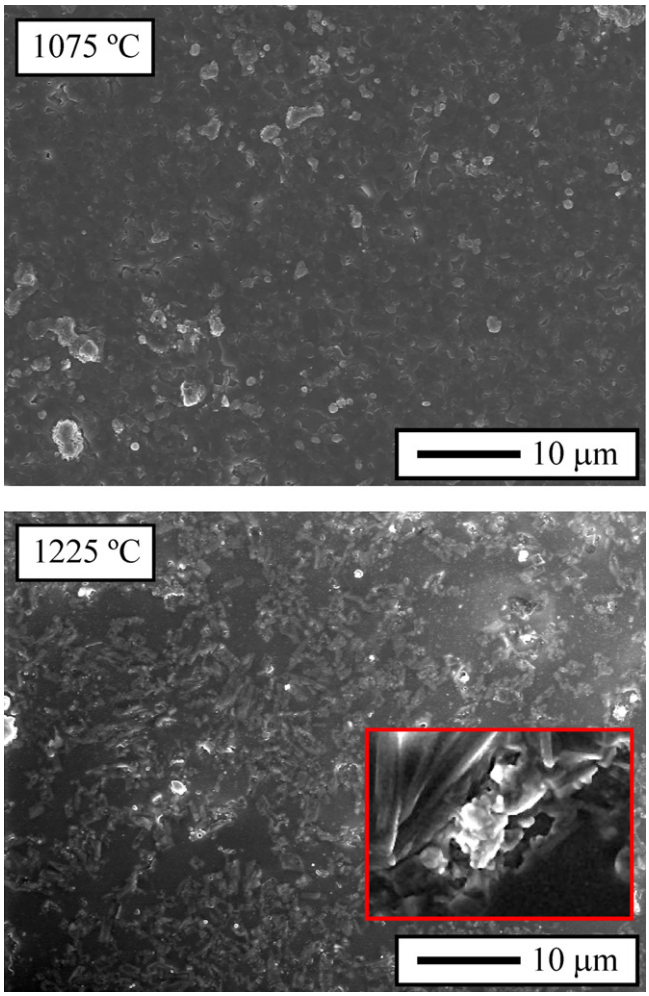

Fig. 6. Plane-view SEM micrographs (taken with backscattered electrons) of the PLPS SiC–Sc ceramic after oxidation in oxygen for 22 h at: (A) 1075 °C, and (B) 1225 °C. The insert is a higher-magnification SEM micrograph of the crystals.

The origin of the anomalous oxidation behaviour established from the PLPS SiC–Gd ceramic study is also valid for the rest of PLPS SiC ceramics. Certainly, the SEM observations of the oxide scales in the PLPS SiC–Sc and –Sm ceramics such as those shown in Figs. 6 and 7 confirm the marked difference in the coverage of the oxide scale by crystals when the oxidizing temperature rises above 1100 °C. One thus concludes that not only is anomalous oxidation a universal property of all PLPS SiC ceramics, but its origin is also common to them all. The difference between the PLPS SiC ceramics fabricated with different rare-earth oxides is then simply that the temperature of occurrence of the anomalous oxidation will vary within the range 900–1150 °C in keeping with the crystallization temperatures of the corresponding rare-earth silicates.

Finally, the present study has interesting implications concerning the utilization of PLPS SiC ceramics in air or other oxidizing atmospheres at moderate temperatures (i.e., <1100 °C). Indeed, according to these results and analyses it does not seem very practical to use them directly in the as-processed condition due to their poor oxidation resistance.

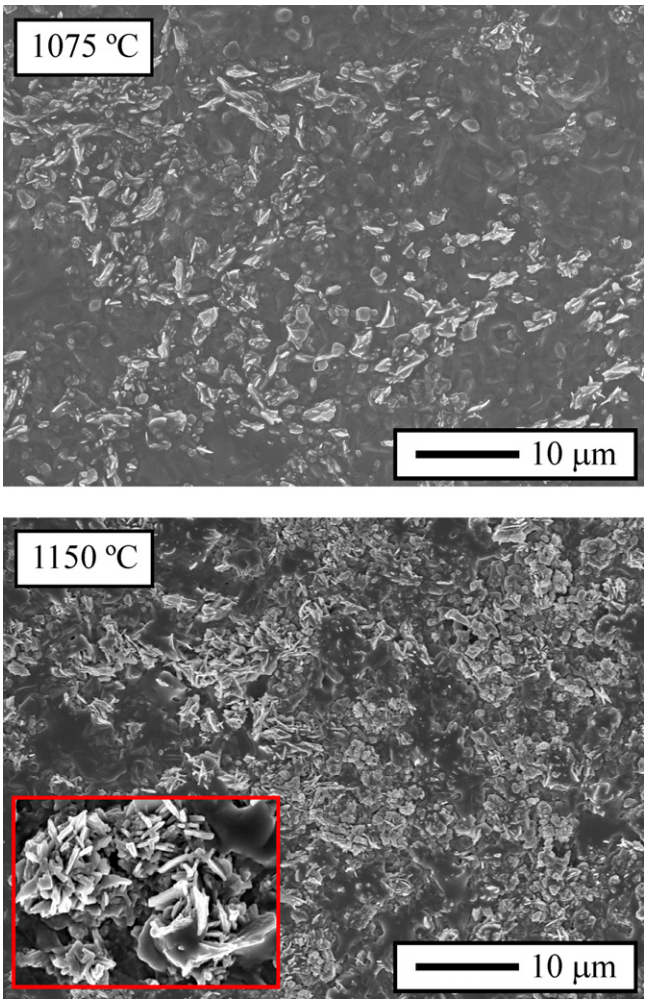

Fig. 7. Plane-view SEM micrographs (taken with backscattered electrons) of the PLPS SiC–Sm ceramic after oxidation in oxygen for 22 h at: (A) 1075 °C, and (B) 1150 °C. The insert is a higher-magnification SEM micrograph of the crystals.

On the contrary, it would be advisable to pre-oxidize them at temperatures around 1100–1150 °C (depending on the specific rare-earth oxides used as sintering additives) for about 0.5 h or so to induce the formation of an oxide scale riddled with crystalline rare-earth silicates that will act as barriers against oxidation. When then used below 1100 °C, the combination of the lower diffusion coefficients of oxygen at these temperatures together with the reduced cross section available for the inward diffusion of oxygen will provide these ceramics with the superior oxidation resistance they do not currently have. This strategy may also be applicable to other SiO_2-scale-forming ceramics that have been sintered using rare-earth oxides, as for example PLPS Si_3N_4, although this possibility remains to be confirmed by further oxidation studies.

4. Concluding remarks

It has long been believed that the oxidation resistance of PLPS SiC within the passive and protective oxidation regime scales inversely with temperature. However, here we have presented contrary evidence demonstrating that the oxidation behaviour is actually universally anomalous, with an oxidation resistance that does not decrease continuously with increasing oxidizing temperature. In particular, the thermobalance oxidation of PLPS SiCs processed with Al_2O_3–Gd_2O_3, Al_2O_3–Sc_2O_3, or Al_2O_3–Sm_2O_3 revealed the existence of much less oxidation above 1100 °C than below, an unexpected phenomenon that had been observed before for the furnace oxidation of a PLPS SiC processed with Al_2O_3–Y_2O_3. By characterizing the oxide scales through SEM, EDXS, and XRD, and modeling the oxidation curves by the parabolic and arctan rate laws, we established that the origin of the anomalous oxidation behaviour is the crystallization within the oxide scale of rare-earth silicates that markedly reduce the effective cross section available for inward diffusion of oxygen, thus notably improving the oxidation resistance. This anomalous oxidation behaviour would seem to be inevitable in other SiO_2-scale-forming ceramics that have been sintered using rare-earth oxides, as for example LPS Si_3N_4, although this assumption requires experimental confirmation. Finally, based on the results and analyses, it emerges that if the PLPS SiC ceramics are to be used at moderate temperatures (i.e., <1100 °C) in air or other oxidizing atmosphere, they require pre-oxidization at 1100–1150 °C for about 0.5 h or so to promote the formation of the crystalline oxide scale that provides them with the superior oxidation resistance they do not have in the as-processed condition.

Acknowledgements

This work was partly supported by the Ministerio de Ciencia y Tecnología (Government of Spain) and FEDER funds under Grants No. MAT 2007-61609 and MAT2010-16848.

References

1. Meetham GW, Van de Voorde MH. *Materials for high temperature engineering applications*. New York: Springer; 2000.
2. Nickel KG. Corrosion of advanced ceramics. Measurement and modelling'. *NATO ASI Series, Series E (Appl Sci)* 1994;**267**.
3. Fordham RJ. *High temperature corrosion of technical ceramics*. London: Elsevier Applied Science; 1990.
4. Rodríguez-Rojas F, Ortiz AL, Guiberteau F, Nygren M. Oxidation behaviour of pressureless liquid-phase-sintered α-SiC with additions of $5Al_2O_3 + 3RE_2O_3$ (RE = La, Nd, Y, Er, Tm, or Yb). *J Eur Ceram Soc* 2010;**30**(15):3209–17.
5. Singhal SC. Oxidation kinetics of hot-pressed silicon carbide. *J Mater Sci* 1976;**11**(7):1246–53.
6. Costello JA, Tressler RE. Oxidation-kinetics of hot-pressed and sintered α-SiC. *J Am Ceram Soc* 1981;**64**(6):327–31.
7. Liu D-M. Oxidation of polycrystalline α-silicon carbide ceramic. *Ceram Int* 1997;**23**(5):425–36.
8. Park SC, Cho K, Kim JJ. Oxidation of hot-pressed silicon carbide in the cyclic and static conditions. *J Mater Sci Lett* 1998;**17**(1):23–5.
9. Baxter D, Bellosi A, Monteverde F. Oxidation and burner rig corrosion of liquid phase sintered SiC. *J Eur Ceram Soc* 2000;**20**(3):367–82.
10. Chartier T, Laurent JM, Smith DS, Valdivieso F, Goeuriot P, Thevenot F. Oxidation resistance and electrical properties of silicon carbide added with Al_2O_3, AlN, Y_2O_3 and NiO. *J Mater Sci* 2001;**36**(15):3793–800.
11. Choi HJ, Lee JG, Kim YW. Oxidation behavior of liquid-phase sintered silicon carbide with aluminum nitride and rare-earth oxides. *J Am Ceram Soc* 2002;**85**(9):2281–6.

12. Guo S, Hirosaki N, Tanaka H, Yamamoto Y, Nishimura T. Oxidation behavior of liquid-phase sintered SiC with AlN and Er_2O_3 additives between 1200 °C and 1400 °C. *J Eur Ceram Soc* 2003;**23**(12): 2023–9.
13. Biswas K, Rixecker G, Aldinger F. Improved high temperature properties of SiC-ceramics sintered with Lu_2O_3-containing additives. *J Eur Ceram Soc* 2003;**23**(7):1099–104.
14. Biswas K, Rixecker G, Aldinger F. Effect of rare-earth cation additions on the high temperature oxidation behavior of LPS–SiC. *Mater Sci Eng* 2004;**A374**(1-2):56–63.
15. Weidenmann KA, Rixecker G, Aldinger F. Liquid phase sintered silicon carbide (LPS–SiC) ceramics having remarkably high oxidation resistance in wet air. *J Eur Ceram Soc* 2006;**26**(13):2453–7.
16. Rodríguez-Rojas F, Borrero-López O, Ortiz AL, Guiberteau F. Oxidation kinetics of pressureless liquid-phase-sintered α-SiC in ambient air at elevated temperatures. *J Mater Res* 2008;**23**(6):1689–700.
17. Rodríguez-Rojas F, Ortiz AL, Borrero-López O, Guiberteau F. Effect of Ar or N_2 sintering atmosphere on the high-temperature oxidation behaviour of pressureless liquid-phase-sintered α-SiC in air. *J Eur Ceram Soc* 2010;**30**(1):119–28.
18. Jensen RP, Luecke WE, Padture NP, Wiederhorn SM. High-temperature properties of liquid-phase-sintered α-SiC. *Mater Sci Eng* 2000;**A282**(1-2):109–14.
19. Xu H, Bhatia T, Deshpande SA, Padture NP, Ortiz AL, Cumbrera FL. Microstructural evolution in liquid-phase-sintered SiC. Part I: effect of starting powder. *J Am Ceram Soc* 2001;**84**(7):1578–84.
20. Rodríguez-Rojas F, Ortiz AL, Borrero-López O, Guiberteau F. Effect of the sintering additive content on the non-protective oxidation behaviour of pressureless liquid-phase-sintered α-SiC in air. *J Eur Ceram Soc* 2010;**30**(6):1513–8.
21. Kępiski L, Wołcyrz M. Nanocrystalline rare earth silicates: structure and properties. *Mater Chem Phys* 2003;**81**(2-3):396–400.